

Supplementary Information for

**Digital microfluidics with impedance sensing for integrated cell culture and analysis**

Steve C.C. Shih,<sup>1,2</sup> Irena Barbulovic-Nad,<sup>1,2</sup> Xuning Yang,<sup>3</sup> Ryan Fobel,<sup>1,2</sup>

Aaron R. Wheeler<sup>1,2,4†</sup>

<sup>1</sup> Institute for Biomaterials and Biomedical Engineering, University of Toronto, 164 College St., Toronto, ON, M5S 3G9

<sup>2</sup> Donnelly Centre for Cellular and Biomolecular Research, 160 College St., Toronto, ON, M5S 3E1

<sup>3</sup> Department of Engineering Science, University of Toronto, 35 St George St., Toronto, ON, M5S 1A4

<sup>4</sup> Department of Chemistry, University of Toronto, 80 St George St., Toronto, ON, M5S 3H6

† Corresponding Author  
email: [aaron.wheeler@utoronto.ca](mailto:aaron.wheeler@utoronto.ca)  
tel: (416) 946 3864  
fax: (416) 946 3865

**Keywords:** digital microfluidics, cell impedance, multiplexing, adherent cells, electrowetting

## **DMF device fabrication**

Devices were fabricated in the University of Toronto Emerging Communications Technology Institute (ECTI) cleanroom facility. Fabrication reagents and supplies included Parylene-C dimer from Specialty Coating Systems (Indianapolis, IN, US), gold- and chromium-coated glass slides from Telic (Valencia, CA), indium tin oxide- (ITO) coated glass slides (Delta Technologies Ltd, Stillwater, MN), Teflon-AF from DuPont (Mississauga, ON), Shipley S1811 photoresist and MF-321 photoresist developer from Rohm and Haas (Marlborough, MA), Standard KI/I<sub>2</sub> gold etchant was from Sigma, CR-4 chromium etchant was from OM Group (Cleveland, OH), and AZ-300T photoresist stripper from AZ Electronic Materials (Somerville, NJ).

DMF device bottom-plates bearing patterned electrodes and contact pads were formed by photolithography and etching. Briefly, gold- and chromium-coated substrates were spin-coated with S1811 photoresist (3000 rpm, 30 s). The substrates were pre-baked on a hot-plate (100°C, 2 min) and exposed to UV through a photomask printed at Pacific Arts and Design (Markham, ON) for 10 s (30 mW cm<sup>-2</sup>) and then developed by immersing in MF-321 for ~3 min. Gold was etched by immersing in gold etchant (~5 min), followed by chromium etching by immersing in CR-4 (~10 s). Substrates were then immersed in AZ 300T (5 min) to remove the photoresist and finally washed in DI water and dried under a stream of nitrogen. These devices were then coated with 2 μm of Parylene-C and 50 nm of Teflon-AF. Parylene-C was applied using a vapor deposition instrument (Specialty Coating Systems), and Teflon-AF was spin-coated (1% wt/wt in Fluorinert FC-40, 1000 rpm, 30 s) followed by post-baking on a hot-plate (160°C, 10 min). Dicing tape was placed on the electrode contact pads prior to parylene coating and was removed after Teflon-AF coating to facilitate electrical contact. As depicted in Fig 1a in the main text, each bottom plate

features an array of 66 electrodes, including six reservoir electrodes ( $\sim 34.8 \text{ mm}^2$  area), six active dispensing electrodes ( $\sim 6.37 \text{ mm}^2$  area), and 54 driving electrodes ( $\sim 4.88 \text{ mm}^2$  area). As shown, six of the driving electrodes served dual-purposes, also acting as cell-sensor electrodes. The electrode array has inter-electrode gaps of 30-100  $\mu\text{m}$ , and each electrode is connected to an array of contact pads on the side of the device spaced appropriately to interface with a 40-pin connector (Compar Inc., Burlington ON).

DMF device top-plates were formed from ITO-glass substrates coated with 50 nm Teflon-AF using the same procedure described for bottom plates (as above). The Teflon-AF was patterned by lift-off to feature six 1 mm diameter circular regions of exposed ITO (known as “cell-culture sites”) spaced 9 mm apart using methods described previously (Eydelnant et al. 2012). As shown in Fig. 1b in the main text, devices were assembled with an ITO-glass top plate and a gold-on-glass bottom plate separated by a spacer formed from 2 pieces of double-sided tape (total thickness of 180  $\mu\text{m}$ ), such that each cell culture site on the top plate was aligned over a cell-sensor electrode. Moreover, each 25 mm x 75 mm top plate was roughly aligned with the outer-edges of the reservoir electrodes on the bottom plate.

### **DMF device operation**

80-120  $V_{\text{RMS}}$  droplet driving potentials were generated by amplifying the sine wave output of a function generator (Agilent Technologies, Santa Clara, CA) operating at 15 kHz. The application of driving potentials was managed using an automated feedback control system for high-fidelity droplet manipulation (Shih et al. 2011) using a circuit described in detail elsewhere (Shih et al. 2012). As shown in Figure S1, the top plate electrode is connected to a 1  $\mu\text{F}$  capacitor, a voltage clamp (two 1N4007 diodes, Creatron Inc, Toronto, ON), and an AD5206 digital

potentiometer (Analog Devices, Brampton, ON, Canada). To move a droplet onto a given destination electrode on the bottom plate, a 505 ms pulse of driving potential is applied to the destination electrode relative to the top-plate electrode. During the final 5 ms of the voltage pulse, the potentiometer is triggered to deliver 5% of the voltage to the positive terminal of a buffered op-amp (MCP6004, Microchip, Brampton, ON, Canada), the output of which is connected to the analog input of an RBBB Arduino microcontroller (Modern Device, Providence, RI). The magnitude of the output voltage,  $V_{\text{sense}}$ , is proportional to the impedance of the volume between the destination electrode on the bottom plate and the top plate electrode. For example unit droplets of DI water have  $V_{\text{sense}} = 243.6 \pm 2.4$  mV, and virtual microwells have  $V_{\text{sense}} = 43.6 \pm 2.9$  mV. Similar values were recorded (for use as a threshold value) for each of the liquids used here. After each voltage pulse, the driving software compares the measured impedance to the threshold value, and if the measured impedance is below the threshold, additional voltage pulses are triggered with +10  $V_{\text{RMS}}$  higher magnitudes until the droplet completes the desired operation. The same system was also used to make impedance measurements on adherent cells, as described below.

### **Droplet operations and programs**

Five droplet operations were used in the experiments described here. In droplet operation one, *reservoir loading*, an 8  $\mu\text{L}$  aliquot of reagent was pipetted onto the bottom plate at the edge of the top plate, and loaded by applying driving potential to the appropriate reservoir electrode (colored blue in Fig. 1 in the main text) to draw the fluid into the reservoir. In droplet operation two, *active dispensing*, a  $\sim 1$   $\mu\text{L}$  “unit droplet” was formed on an active dispensing-electrode (colored green in Fig. 1 in the main text) by pulling and necking from the reservoir as described

previously (Cho et al. 2003). In droplet operation three, *active mixing*, two 1  $\mu\text{L}$  unit droplets were merged and the combined 2  $\mu\text{L}$  droplet was shuttled back and forth across 10 electrodes 10 times. In droplet operation four, *active splitting*, a combined 2  $\mu\text{L}$  droplet was split into two unit droplets as described previously (Cho et al. 2003). In droplet operation five, *passive dispensing*, a 1  $\mu\text{L}$  unit droplet was actuated across a cell culture site (on the top plate, above a red cell-sensor electrode, in Fig. 1 in the main text), generating a  $\sim 0.2$   $\mu\text{L}$  sub-droplet (or “virtual microwell”) as described previously (Eydelnant et al. 2012). The latter process was used both to generate virtual microwells on dry cell culture sites, and to displace the contents of existing virtual microwells on sites bearing droplets from previous operations.

Four programs were used in the work described here, comprising combinations of the five operations described above. Program one, *cell seeding*, was used for fresh devices without cells or virtual microwells, and was implemented in three steps (S1-S3). In step (S1), one or more aliquots of cells suspended in media were loaded into the appropriate reservoirs. In step (S2), one or more unit droplets of cells in suspension were actively dispensed onto the array of electrodes. If more than one unit droplet was to be dispensed from a given reservoir, after each dispensing step, the (old) reservoir volume was removed by wicking with a tissue and replaced with (new) aliquot of cells by repeating (S1). In step (S3), a virtual microwell was generated on a dry cell culture site from each of the unit droplets generated in (S2), and the remainders of the unit droplets were driven to (a) waste reservoir(s). The remaining contents of all reservoirs were removed with a tissue.

Program two, *cell culture*, was used for devices with cells in virtual microwells, and was implemented in two steps (C1-C2). In step (C1), the device was flipped upside down as described previously (Srigunapalan et al. 2012) (i.e., with the top plate on the bottom) and stored an

incubator at 37°C. In step (C2), the device was removed from the incubator and returned to its normal orientation (i.e., with top plate on top).

Program three, *reagent exchange*, was used for devices with cells in virtual microwells, and was implemented in three steps (E1-E3). In step (E1), one or more aliquots of a given reagent were loaded into the appropriate reservoirs. In step (E2), two or more unit droplets of reagent were actively dispensed. If more than four droplets were to be dispensed from a given reservoir, (E1) was repeated after the four dispensing steps to refill the reservoir. In step (E3), the (old) contents of each virtual microwell were replaced with (new) reagent by sequentially passive dispensing two unit droplets onto each cell culture site. The remainders of the unit droplets were driven to (a) waste reservoir(s), and the contents of all reservoirs were removed with a tissue.

Program four, *dilution and exchange*, was used for devices with cells in virtual microwells, and was implemented in nine steps (D1-D9). In step (D1), one aliquot each of a reagent and a diluent were loaded into different reservoirs. In step (D2), one 1  $\mu\text{L}$  unit droplet each of reagent and diluent were actively dispensed, then (D3) actively merged and mixed, and then (D4) actively split into two mixed unit droplets. One of the mixed unit droplets was saved for future steps, and in step (D5), the (old) contents of a virtual microwell were replaced with (new) mixed unit droplet onto a cell culture site. The remainder of the unit droplet was driven to a waste reservoir. In step (D6), a fresh 1  $\mu\text{L}$  unit droplet of diluent was actively dispensed, and then (D7) actively merged and mixed with the saved 1  $\mu\text{L}$  unit droplet (from step D4, above). Steps (D8-D9) were then implemented, which were repeats of (D4-D5). Steps (D6-D9) were then repeated until each cell culture site had been exchanged with a constituent in the dilution series. At the end of the process, the contents of all reservoirs were removed with a tissue.

## Cell impedance model

A circuit was developed to model the impedance of the system, building from similar work by Morgan and coworkers (Morgan et al. 2007; Sun and Morgan 2010; Sun et al. 2010). The circuit is shown in Table S1 and has four elements in series. The first element represents the parylene insulator on the bottom-plate of the device, modeled as a capacitor ( $C_i$ ). The second element represents the bulk droplet, modeled as a resistor and a capacitor ( $R_{\text{liq\_bulk}}$  and  $C_{\text{liq\_bulk}}$ ) in parallel. The third element represents the interface between the droplet and the top-plate electrode (arbitrarily chosen to be 10  $\mu\text{m}$  thick), and contains two sub-circuits (in parallel). The first sub-circuit represents the cells at the interface, with each cell modeled as two capacitors and a resistor ( $C_{\text{mem}}$ ,  $R_{\text{cyto}}$ ,  $C_{\text{mem}}$ ) for  $N_c$  cells in parallel. The second sub-circuit represents the liquid at the interface, modeled as a resistor and a capacitor ( $R_{\text{liq\_int}}$  and  $C_{\text{liq\_int}}$ ) in parallel. The fourth circuit element represents the potentiometer and the internal capacitance of the op-amp ( $R_{\text{pot}}$ , and  $C_{\text{op}}$ ) in the measurement circuit. The circuit model does not include representations of cell membrane resistance or cytoplasm capacitance, the 1  $\mu\text{F}$  coupling capacitor, or the resistance or capacitance of the thin layers of Teflon-AF, which are assumed to have negligible effects.

The electrical properties of each element in the circuit model are listed in Table S1. Values that were not known, measured, or found in the literature were calculated according to equations 1 and 2,

$$R = \frac{\rho t}{A} \quad \text{Eq. 1}$$

$$C = \frac{\epsilon_0 \epsilon_r A}{t} \quad \text{Eq. 2}$$

where  $t$ ,  $A$ ,  $\rho$ , and  $\epsilon_r$  are the thickness, area, resistivity, and dielectric constant of the material, and  $\epsilon_0$  is the permittivity of free space.  $V_{\text{sense}}$  as a function of frequency (0-35 kHz) was simulated

using LTSpice (Linear Technology, Milipitas, CA) with a 100 V<sub>RMS</sub> sinusoidal source. The simulated data for four conditions (cell media/high cell density, cell media/low cell density, sucrose/high cell density, sucrose/low cell density) were compared with experimental measurements (described above).

## References

- Cho, S.K., Moon, H.J., Kim, C.J., 2003. *Journal of Microelectromechanical Systems* 12, 70-80
- Eydelnant, I.A., Uddayasankar, U., Li, B., Liao, M.W., Wheeler, A.R., 2012. *Lab on a Chip* 12, 750-757
- Morgan, H., Sun, T., Holmes, D., Gawad, S., Green, N.G., 2007. *J. Phys. D: Appl. Phys.* 40, 61-70
- Shih, S.C.C., Fobel, R., Kumar, P., Wheeler, A.R., 2011. *Lab on a Chip* 11, 535-540
- Shih, S.C.C., Yang, H., Jebrail, M.J., Fobel, R., McIntosh, N., Al-Dirbashi, O.Y., Chakraborty, P., Wheeler, A.R., 2012. *Analytical Chemistry* 84, 3731-3738
- Srigunapalan, S., Eydelnant, I.A., Simmons, C.A., Wheeler, A.R., 2012. *Lab on a Chip* 12, 369-375
- Sun, T., Morgan, H., 2010. *Microfluid Nanofluid* 8, 423-443
- Sun, T., Swindle, E.J., Collins, J.E., Holloway, J.A., Davies, D.E., Morgan, H., 2010. *Lab on a Chip* 10, 1611-1617

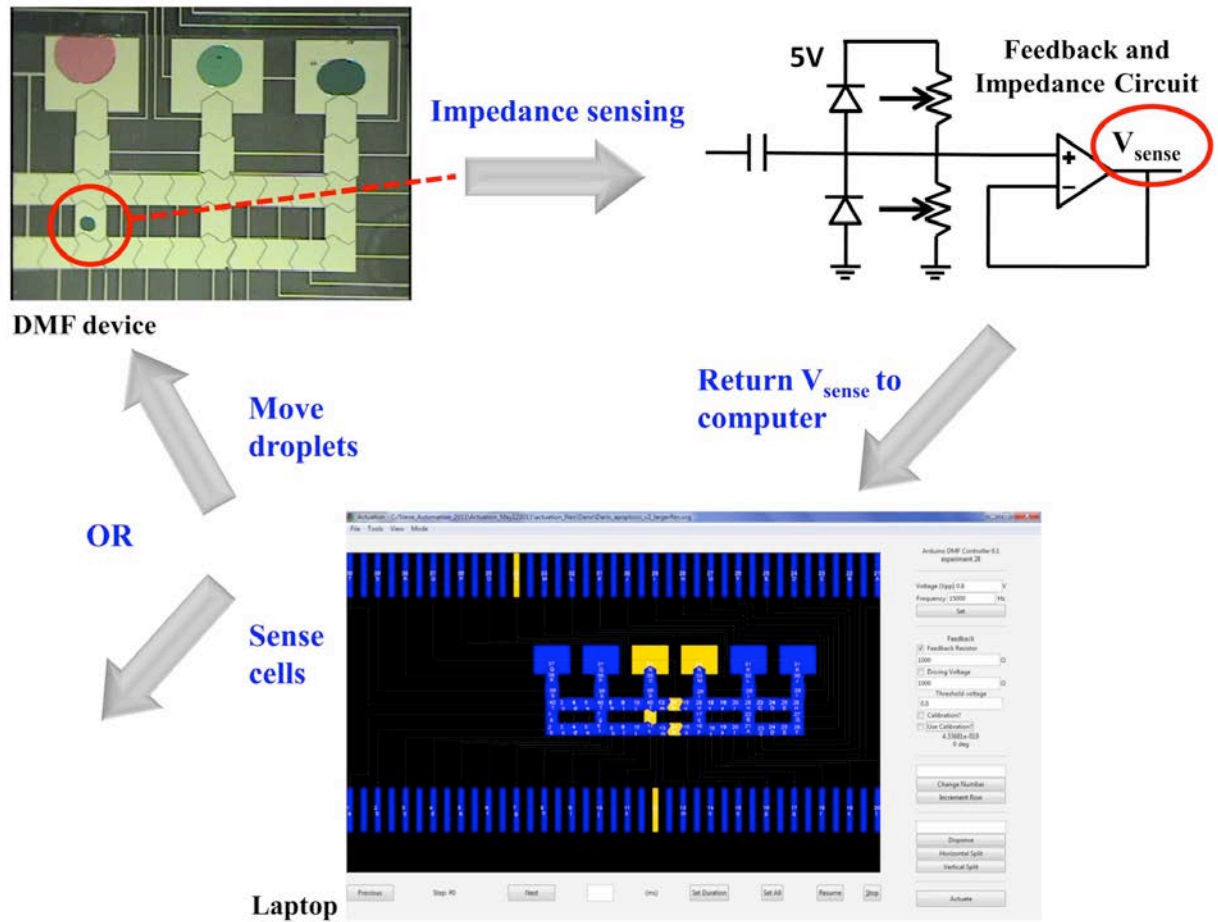
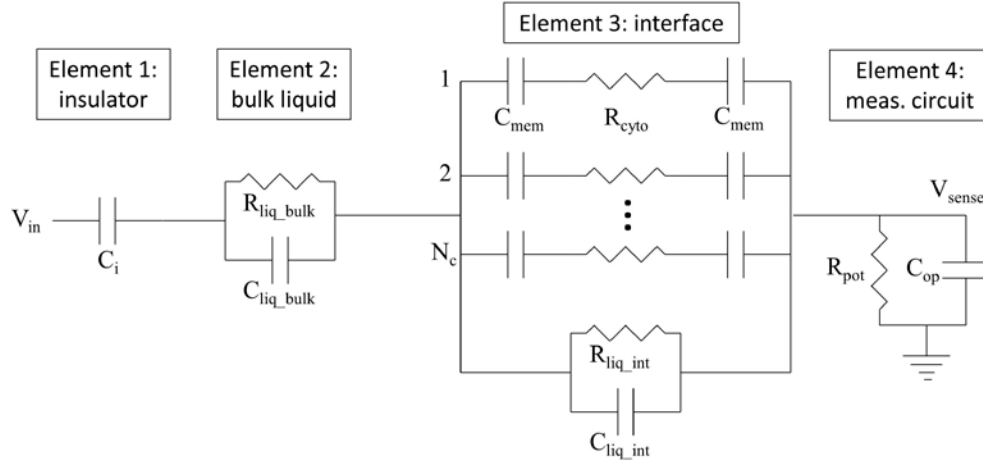


**Figure S1** – Impedance measurement circuit. The circuit was used for two purposes: droplet control and cell sensing. For droplet control,  $V_{sense}$  is measured during droplet manipulation to enable feedback control over unit droplet position (Shih et al. 2011). For cell sensing,  $V_{sense}$  is measured in static virtual microwells positioned over cell-sensing electrodes.

**Table S1:** Model circuit and values used in LTSPICE simulations.



Item	Circuit Element	Value	Reference or measured	Equation and Parameters
Element 1: insulator	$C_i$	10.4 pF	N/A	Eq. 2; $\epsilon_r = 3.0$ ; $t = 2 \mu\text{m}$ ; $A = 0.785 \text{ mm}^2$
Element 2: bulk liquid	$R_{\text{liq\_bulk}}$	cell media: 400 $\Omega$	measured	N/A
		sucrose: 1.8 M $\Omega$	measured	N/A
	$C_{\text{liq\_bulk}}$	cell media: $\sim 0$ pF	N/A	N/A
		sucrose: 19.5 pF	measured	N/A
Element 3: interface	$C_{\text{mem}}$	$0.785 \text{ pF} \cdot \text{cell}^{-1}$	(Morgan et al. 2007; Sun and Morgan 2010)	N/A
	$R_{\text{cyto}}$	$212 \text{ k}\Omega \cdot \text{cell}^{-1}$	(Morgan et al. 2007; Sun and Morgan 2010)	Eq. 1; $\rho = 1.67 \Omega \cdot \text{m}$ ; $t = 10 \mu\text{m}$ ; $A = 7.85 \times 10^{-5} \text{ mm}^2$
	$R_{\text{liq\_int}}$	cell media: 22.9/26.7** $\Omega$	N/A	Eq. 1; $\rho = 1.74 \Omega \cdot \text{m}^*$ ; $t = 10 \mu\text{m}$ ; $A = 0.785 \text{ mm}^2 - A_c$
		sucrose: 103/121** k $\Omega$	N/A	Eq. 1; $\rho = 7850 \Omega \cdot \text{m}^*$ ; $t = 10 \mu\text{m}$ ; $A = 0.785 \text{ mm}^2 - A_c$
	$C_{\text{liq\_int}}$	cell media: $\sim 0$ pF	N/A	N/A
sucrose: 54.6/46.1** pF		N/A	Eq. 2; $\epsilon_r = 80$ ; $t = 10 \mu\text{m}$ ; $A = 0.785 \text{ mm}^2 - A_c$	
Element 4: meas. circuit	$R_{\text{pot}}$	12 k $\Omega$	N/A	N/A
	$C_{\text{op}}$	20 pF	N/A	N/A

\*  $\rho$  extrapolated from measured  $R_{\text{liq\_bulk}}$

\*\* Values for low and high cell density